Onboard Real-Time Navigation for the Sentinel-3 Mission

O. Montenbruck, A.Hauschild, *Deutsches Zentrum für Luft- und Raumfahrt (DLR/GSOC)*
F. Zangerl, W. Zsalcsik, *RUAG Aerospace Austria (RAA)*
P. Ramos-Bosch, *Technical University of Catalonia (UPC)*
U. Klein, *European Space Agency (ESA/ESTEC)*

BIOGRAPHIES

Dr. Oliver Montenbruck is head of the GNSS Technology and Navigation Group at DLR's German Space Operations Center, where he started to work as a flight dynamics analyst in 1987. His current research activities comprise space-borne GNSS receiver technology, autonomous navigation systems, spacecraft formation flying and precise orbit determination.

André Hauschild received his diploma degree in mechanical engineering in March 2007 from the Technical University of Braunschweig, Germany, and subsequently became a Ph.D. candidate at DLR's German Space Operations Center. His research focuses on real-time clock-offset estimation for the GPS constellation.

Franz Zangerl received his masters degree in electrical engineering from the Technical University of Vienna in 1990. He is leader of the processing system group at RUAG Aerospace Austria (former Austrian Aerospace). Since 1997 is working as system engineer in the area of GNSS receivers for space applications.

Wolfgang Zsalcsik received his degree in electrical engineering from the Technical Highschool in Mödling in 1991. He is Senior Design Engineer at RUAG Aerospace Austria. His activities covered hardware-, software-, ASIC/FPGA- and test system design for various missions including GRAS, Galileo, SWARM and Sentinel.

Dr. Pere Ramos-Bosch works as a GNSS researcher in the group of Astronomy and GEomatics (gAGE) belonging to the Technical University of Catalonia (UPC). He received his PhD degree in Aerospace Science & Technology in 2008, his diploma in Telecommunications Engineering in 2004 (both from UPC), and his diploma in Physics from the University of Barcelona in 2006.

Dr. Ulf Klein received his PhD in 1993 from University of Bremen where he headed the research group for ground-based microwave observation of atmospheric trace gases and lectured courses until 2001. He then joined ESA developing new technologies and missions for spaceborne Earth observation. In 2007 he moved to the Sentinel-3 project within ESA taking care of the missions microwave radiometers and it's precise orbit determination systems.

ABSTRACT

The paper discusses the design of the GPS real-time navigation system for the Sentinel-3 mission and presents its validation using signal-simulator test data as well as GPS flight data from the GRAS receiver on MetOp. Trade-offs between accuracy, robustness and run-time performance are discussed taking into account the specifics of the Sentinel-3 mission. It is demonstrated that a 1m 3D rms position accuracy and a better than 0.5 m radial accuracy can be achieved during routine operations. Further attention is given to the robust handling of orbit correction maneuvers with minimum operational implications.

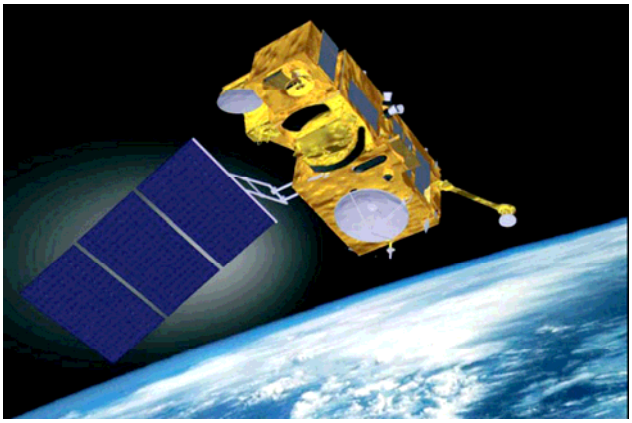

Fig. 1 The Sentinel-3 spacecraft (Artist's impression)

INTRODUCTION

The Sentinel-3 Mission [1] is part of ESA's Global Monitoring for Environment and Security program (GMES). The mission will comprise a total of 4 spacecrafts to provide ocean monitoring capabilities for up to 20 years and ensure a continuity of service after the end of ENVISAT. The Sentinal-3 spacecrafts (Fig. 1) will have a mass of roughly 1200 kg and will be placed into a Sun-synchronous orbit of 800 km altitude. Key instruments comprise an altimeter, a Microwave Radiometer (MWR), a Sea & Land Surface Temperature (SLST) instrument, and the Ocean/Land Colour Imager (OLCI). Navigation requirements in the Sentinel-3 mission are driven by the altimeter operation and data analysis. Specifically, a 2-3 cm radial accuracy is required for the final post-facto orbit reconstruction to enable an

accurate monitoring of the ocean surface height. In real-time, a better than 3 m radial position (RMS) knowledge is, furthermore, required to support an open-loop operation mode of the altimeter.

To meet these mission needs, each Sentinel-3 spacecraft will be equipped with a cold-redundant pair of dual-frequency GPS receivers. The model selected for the Sentinel-3 mission represents an advanced version of the GPS precise orbit determination (POD) receiver developed by RAA for various other ESA Earth observation missions. Similar to the GRAS instrument on MetOp, the receiver makes use of the AGGA-2 Advanced GPS/GLONASS ASIC correlator chip [3]. With a total of two AGGA-2 chips, the GPS POD receiver can process a total of 24 single frequency channels or, equivalently, eight dual-frequency channels. The R/F frontend uses down-converters and 50 MHz A/D-converters with 3 bits resolution that have both been developed by NEMERIX for use in spaceborne GNSS receivers and offer a high level of radiation tolerance (100 krad total dose and 70 MeV/mg/cm2 for heavy ions). The reference frequency for the GPS POD receiver is obtained from a 10 MHz OCXO that offers a low drift rate and high stability. The correlator control, signal tracking and navigation solution computation as well as the telemetry and telecommand processing within the GPS POD receiver is performed by a LEON 32-bit micro-processor. At a mass of less than 3 kg (excluding harness and antenna) the receiver fits into an envelope of 32 x 24 x 10 cm3 and requires a power of 10 W at steady state conditions.

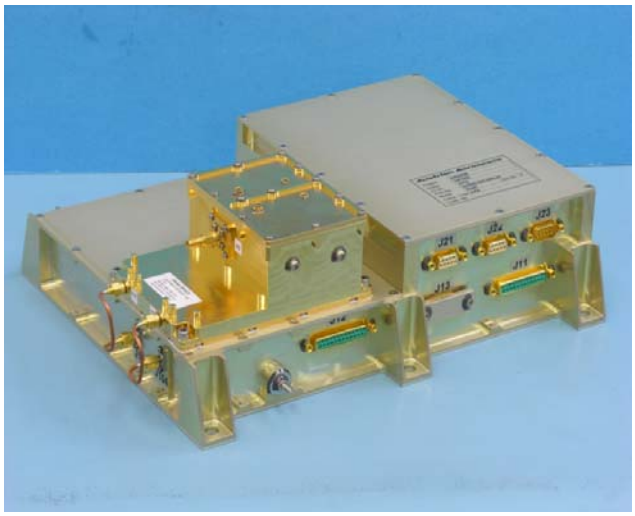

Fig. 2 Engineering model of the RAA GPS POD receiver ([2])

Due to gain and field-of-view limitations of the employed GPS antenna, a robust real-time navigation performance is hard to guarantee with a purely kinematic dual-frequency solution based on pseudorange measurements. For Sentinel-3, the GPS POD receiver will therefore be upgraded with a real-time navigation software that performs a dynamical filtering of raw GPS measurements. Algorithmic details are presented in the following section, which discusses both a pseudorange-only filter design (the current baseline) and an advanced formulation with additional use of carrier phase measurements. Special attention is given to the handling of maneuvers in the real-time navigation filter which minimizes the downtime of the spacecraft for science data takes. In the subsequent section the tracking and measurement performance of the Sentinel-3 POD receiver is assessed based on a signal simulator test with the current prototype receiver model. Finally, the performance of the real-time navigation algorithm is validated for maneuver-free and maneuver-inclusive data arcs making use of the raw measurements collected in the signal simulator test. For added realism, actual flight data from the GRAS instrument on MetOp are also analyzed.

REAL-TIME NAVIGATION ALGORITHMS

A reference algorithm for real-time navigation based on raw GPS measurements has earlier been described in [4] and successfully implemented in DLR's Phoenix-XNS receiver for the PROBA-2 [5] and X-Sat missions. For use in Sentinel-3, the generic filter design and parameter settings are adapted to the specific receiver capabilities and the mission requirements. In particular, a ionosphere-free combination of dual-frequency measurements is employed and the filter can be operated at a 1 Hz update due to the powerful LEON processor core. A key extension of the previous design is the incorporation of maneuvers with minimum impact on the algorithmic and operational complexity.

Dynamical Model

The real-time navigation system for Sentinel-3 is built on a high-grade trajectory model which takes into account the asphericity of the Earth, luni-solar perturbations, as well as drag and solar radiation pressure. Details of the adopted models are described in [6] and references therein. For practical purposes, a 30 x 30 gravity field model has been found appropriate for remote sensing satellites at 800 km altitude. Only at much lower altitudes of about 400 km the use of a 50 x 50 model may be required to achieve a meter-level or better accuracy. Short analytical series expansions are used to compute the lunar and solar coordinates with typical accuracies of 1' to 5', which is fully appropriate for the modeling of the respective third-body perturbations. Drag and solar radiation pressure are described through cannon-ball models and the atmospheric density is computed from a Harris-Priester model for mean solar activity. No upload of solar and geomagnetic activity data is foreseen, since differences between the modeled and actual state of the atmosphere can well be compensated through adjustable filter parameters. Besides a drag and radiation pressure coefficient, these parameters include empirical accelerations in radial, along-track and cross-track direction which helps to compensate any deficiencies of the deterministic force model.

As suggested in [4], an Earth-fixed formulation of the equation of motion has been adopted for the Sentinel-3 navigation system. This choice is based on the consideration that GPS measurements are most conveniently processed in an Earth fixed system that forms the basis for the broadcast ephemerides. Likewise the output of the navigation system is primarily required in an Earth-fixed system that forms the basis for instrument operation and geo-location. Reference system transformations can thus be avoided to a large extend which facilitates a lean implementation and coding of the navigation filter. As an exception, the inertial luni-solar coordinates must be transformed into the Earth-fixed system for modeling the third body perturbations, but only a very moderate accuracy is required in this case. As such, no detailed knowledge of sidereal time and the UT1-UTC offset is required for proper operation of the navigation system. On the other hand, the Earth-fixed formulation of the equation of motion requires the proper consideration of Coriolis and centrifugal accelerations. In particular, the difference between the Earth rotation axis and the z-axis of the WGS84 reference must be known for this purpose, which amounts to typically 0.3", or, equivalently 10 m near the surface of the Earth. For practical purposes it is generally sufficient to update the respective pole coordinates in the Sentinel-3 navigation system once every week through a ground command.

Other than the equation of motion, which accounts for a fairly detailed force model, various simplifications are used for the variational equations. Gravitational forces are only considered up the 2nd order zonal harmonics of the Earth, while luni-solar perturbations can safely be neglected. Compared to a simple linearized form of the state transition matrix that is often used in real-time navigation systems to minimize the computational load, the use of variational equations enables a proper computation of both the state transition and sensitivity matrix irrespective of the integration step and the overall propagation interval.

Between measurement epochs the equation of motion and the associated variational equations are integrated with a 4th order Runge-Kutta (RK4) integrator. Even though the 1s update interval of the Sentinel-3 navigation system would even tolerate a lower order integrator (see [7] for further discussion), the RK4 has been adopted because of its high communality, simple design and sufficient margins for other applications. Furthermore, its use is well compatible with the available processing power of the central processing unit of the GPS receiver.

Measurement Processing and Filter Concept

As a baseline, the Sentinel-3 navigation system processes a ionosphere-free linear combination

$$\rho_{P12} = 2.54 \cdot \rho_{P1} - 1.54 \cdot \rho_{P2}$$

of the P-code pseudoranges on the L1 and L2 frequency. At an average P-code tracking noise of 0.3 to 0.5 m, the linear combination exhibits a noise level of 1 to 1.5 m but is free of ionospheric path delays that affect GPS measurements even at altitudes well above the ionospheric density maximum. The pseudorange provides a direct measure of the distance between receiver and the the GPS satellites except for the unknown receiver clock offset, which is estimated as part of the navigation filter.

The actual measurements are compared against modeled observations, which are computed based on the predicted spacecraft position, the antenna offset from the center-of-mass (assuming a nominal alignment of the s/c with the orbital frame) as well as the GPS position and clock information derived from the broadcast ephemerides. Following a residuals test, which takes into account the propagated state uncertainty and the expected measurements noise covariance, the accepted observations are used to update the filter state.

The filter itself is an extended Kalman filter which combines a time update step with a sequence of scalar measurement updates. Compared to a vector update jointly processing all simultaneous observations, the scalar update minimized the size of the involved vector-matrix operations, does not require dynamical array dimensions and is considered computationally more efficient.

In total, the state vector comprises 12 filter parameters, namely

- the instantaneous spacecraft position and velocity $\boldsymbol{y} = (\boldsymbol{r}, \boldsymbol{v})$,
- the drag (C_D) and radiation pressure (C_R) coefficients,
- the empirical accelerations $\boldsymbol{a}_{emp} = (a_R, a_T, a_N)$ in radial (R), tangential (T), and normal (N) direction,
- and, finally, the receiver clock offset cdt.

Since all measurements are referred to an approximation of GPS time derived from a kinematic navigation solution and a linear clock model, the residual clock offset estimated in the navigation filter is generally a small quantity at the level of 10 m.

The filter is initialized from a kinematic navigation solution which exhibits a representative accuracy of better than 10 m and 10 cm/s once an adequate number (5-6) of GPS satellites is tracked.

Out of the various filter states, the clock offset and the empirical accelerations are treated as stochastic parameters. While a simple white noise model is adequate for the clock state, a Gauss-Markov model has been adopted for the empirical accelerations. It involves an exponential damping of the state during the time update step and the incorporation of process noise in relation to the propagation interval and correlation time scale. The employed parameters are based on a filter tuning performed prior to launch using signal simulator tests and

offline simulations with GPS flight data from other missions. In correspondence with the employed force model simplifications, the amplitude of the empirical accelerations is typically at the level of several 100 nm/s^2 for the along-track and cross-track axis, while much lower values apply for the radial component. Even though the variation of the estimated empirical accelerations does not necessarily resemble that of a Gauss-Markov process, the model has been found to enable a robust and accurate filter performance over a wide range of conditions.

Code and Carrier Filter

As a design alternative, a filter processing both code and carrier phase measurements has been considered in the Sentinel-3 project. Even though the primary mission requirements can well be met with the pseudorange-only filter the incorporation of carrier-phase measurements promises a further improvement in accuracy, a shorter convergence time and an improved performance in case of maneuver. On the other hand the processing of carrier-phase data notably increases the complexity of the filter design and makes it more difficult to perform a reliable data screening. In view of stringent software quality assurance standards, the pseudorange-only filter is therefore considered as a baseline for the Sentinel-3 GPS receiver and navigation system. However, we briefly present its concept and various results within this report to justify the design trade-off and to demonstrate the performance that can ultimately be achieved with a GPS based real-time navigation system.

As is commonly known, carrier phase observations offer a 1000 times smaller measurement noise than pseudoranges, which makes them the preferred choice for high-precision applications. In a spaceborne real-time navigation system, this high accuracy cannot, however, be materialized since the broadcast ephemeris accuracy is much lower and differential GPS real-time navigation is not yet possible for standalone spacecraft. Nevertheless a factor of two performance improvement can still be reached which justifies the increased processing effort for specific applications.

Similar to the pseudorange measurements, a ionosphere-free linear combination is formed from the L1 and L2 carrier phase measurements. It provides an accurate measure of the distance (and clock offset) change over time but suffers from an unknown bias. In the absence of cycle slips, the bias remains constant throughout a continuous tracking arc. Starting from an a priori estimate obtained from the code-carrier difference after initial acquisition, knowledge of the bias can, however, be improved by estimating it within the filter. To this end the filter state is augmented with one bias state per tracking channel. In case of the Sentinel-3 eight channels receiver, a total of 20 states are thus foreseen in the filter state. To avoid a dynamically changing storage allocation, the filter dimension is kept fixed and unused bias state are “frozen” at a zero value if no measurements are collected on the respective tracking channel. The screening of carrier phase measurements proceeds similar to that of the pseudorange measurements but has to account for the variance of the bias in addition to that of the projected position error and clock uncertainty [4]. In case a potential cycle slip is recognized the respective bias state and variance need to be reinitialized. Evidently, only those cycle slips can be detected which are sufficiently large in comparison with the pseudorange, broadcast ephemeris and navigation filter accuracy. On the other hand, small (single cycle) slips that go undetected will not impact the final navigation accuracy in an undue manner.

An interesting aspect of the additional bias states is their ability to partly absorb slowly varying broadcast ephemeris errors. By adding a subtle amount of process noise to the bias state covariance in each time update step, the estimated bias can be allowed to deviate from the theoretical value (i.e. the average code minus carrier difference) and instead minimize the difference between modeled and measured carrier phases, which is partly affected by the ephemeris errors. While some tuning of the respective filter parameters is required for optimum performance, the effectiveness of this approach has extensively been demonstrated and validated with flight data from a variety of space missions [4].

Maneuver Handling

Occasional maneuvers are required in most remote sensing missions to acquire and maintain a desired groundtrack and to counteract secular orbital perturbations. These maneuvers include both in-plane and out-of-plane corrections and may involve velocity increments between a few mm/s and (for orbit acquisition) m/s. For maximum efficiency the thrust is usually directed in flight/anti-flight direction or along the orbital plane normal. Even though a continuous burn would minimize the total maneuver duration, an on-off modulation may be used to avoid excessive thruster heating or to control the net torque during the maneuver when using multiple thrusters. Nevertheless, it is generally adequate to treat the maneuver as a constant net thrust in along-track or cross-track (and, optionally, radial) direction.

Even though a reduced navigation accuracy is generally tolerated during the thrust phase, the real-time navigation system must be able to operate continuously and to rapidly re-acquire its nominal performance after the end of burn. For Sentinel-3, an onboard knowledge of the instantaneous altitude is required for open loop operation of the altimeter and a properly designed maneuver handling will therefore help to avoid potential data acquisition gaps.

Since the dynamical model presented before already accounts for empirical accelerations in RTN direction, it is already well prepared for the incorporation of maneuvers. Based on the planned velocity increment and

total duration, the corresponding acceleration can directly be applied in the propagation of the orbit throughout the thrust arc. However, accelerations between 0.1 mm/s^2 and 5 mm/s^2 may be experienced during Sentinel-3 maneuvers, which exceeds the natural magnitude of the empirical accelerations by 3 to 5 orders of magnitude. Even though it would be possible to adopt the process noise of the empirical acceleration parameter during maneuvers to the magnitude of the thrust acceleration (or at least the uncertainty of the a priori thrust information), this approach was found to degrade the filter performance and the stiffness of the estimated trajectory after the maneuver in an undue manner.

As an alternative, process noise is directly added to the propagated position and velocity in accord with the expected orbit prediction uncertainty due to incomplete knowledge of the maneuver acceleration. Even though this approach cannot provide an estimate of the actual thrust level during the boost phase, it is well suited for the real-time navigation system and delivers reliable position and velocity estimates after the boost end. The increase of the position covariance due to the additional process noise ensures that good measurements are not discarded due to a mismatch of predicted and observed measurements. Furthermore, it makes the filter receptive to new measurements and allows a quick correction of the state vector after the burn end. The robustness of this concept is demonstrated by the fact that it can even cope with a complete lack of a priori Delta-V information, provided that the maneuver start and stop times are known and that a sufficient number of GPS satellites is tracked during the maneuver. In this extreme case, the filter behavior approaches that of a kinematic navigation solution which is mostly measurement driven and relies only moderately on the propagation model. After the boost end, the filter regains its original stiffness and converges back to its steady state navigation performance as soon as a sufficient amount of post-maneuver observations is available.

The choice of suitable process noise settings is again based on pre-mission simulations and performed along with the overall filter tuning. Practical results of the filter performance in the presence of maneuvers are given in a later section of this report following a discussion of the maneuver-free navigation accuracy.

SIGNAL SIMULATOR TESTING

As part of the receiver validation, the tracking and navigation performance of the GPS POD receiver has been assessed with a breadboard model in a dedicated signal simulator test. Even though a Sentinel-3 specific simulation scenario has been defined for this purpose, the test concept closely matches that of previous space receiver tests ([8], [9]). Radio-frequency signal representative of those received by a LEO satellite where generated with a GPS signal simulator (Fig. 3). The receiver telemetry packets were recorded over a 24h data arc and used to generate a RINEX measurement file. Likewise the simulated LEO orbit and GPS ephemeris data were recorded and converted into a standard SP3 file for the subsequent data analysis.

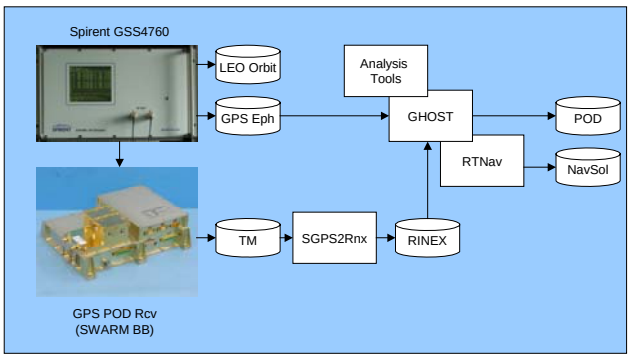

Fig. 3 Signal simulator test concept

Aside from an assessment of the tracking sensitivity and measurement performance the raw measurements were processed with DLR's GPS High Precision Orbit Determination Software Tools (GHOST, [10]) to quantify the receiver contribution to the overall POD accuracy budget. Finally, the recorded measurements were processed in an offline implementation (RTNav) of the real-time navigation filter software to validate the achievable accuracy and perform various design trade-offs prior to the flight software implementation.

The employed test scenario is based on a polar orbit at 800 km altitude for a fictitious epoch in 2014. The Sentinel-3 orbit was numerically integrated using the built-in orbit models of the Spirent simulator. These models are of similar type as the dynamical models of the real-time navigation system but are sufficiently different to ensure a realistic testing. Among others, the Earth gravitational acceleration is computed from a 70x70 JGM-3 model, whereas a more recent GGM01 model up to order 30x30 is employed in the real-time navigation filter.

The GPS constellation has been assumed to comprise 10 Block-IIR satellites and 17 Block-IIF, where the total number of satellites reflects a conservative assumption of the overall GPS availability. Based on the observed performance of the existing IIR satellites, a signal power level of 3dB above the specification was adopted for these satellites in the L1 frequency band, whereas nominal signal levels in accord with [11] were assumed for the IIF satellites. The output power level was raised beyond the specification of the minimum received signal power to compensate the increased noise temperature of the simulator [14] but still yields a fairly conservative carrier-to-noise-density (C/N_0).

In accord with the capabilities of the signal simulator, broadcast ephemeris errors were emulated through constant offsets in radial, tangential and normal direction with an ensemble rms of 1.2 m for each axes. This

magnitude is in good accord with the current Signal-In-Space-Range-Error (SISRE) of about 1 m ([12], [13]) and was found to result in a realistic degradation of the real-time-navigation accuracy. Ionospheric path delays were modelled through a constant vertical total electron content (VTEC) of 10 TECU (10^{17} e^-/m^2) and a Lear mapping function.

For the testing of the real-time navigation performance in the presence of orbital maneuvers, a variant of the scenario with a total of 10 thrust arcs was furthermore defined (Table 1). The simulation covered accelerations between 0.1 and 5.0 mm/s^2, burn durations of 3 to 600 s as well as thrust arcs with on-/off-modulation.

Table 1 Maneuver parameters for Sentinel-3 real-time navigation performance assessment during thrust phases.

Start	Accel [mm/s²]	Direction	Duration [s]	Delta-V [m/s]
02:00:00	0.1	-N	600	0.0600
03:00:00	0.1	+T	600	0.0600
04:00:00	5.0	-N	600	3.0000
05:00:00	5.0	+T	600	3.0000
06:00:00	2.5/5.0	-N	600	2.2500
07:00:00	2.5/5.0	+T	600	2.2500
08:00:00	0.5	-N	15	0.0075
09:00:00	0.5	+T	3	0.0015
10:00:00	0.5	-N	280	0.1400
11:00:00	0.5	+T	25	0.0125

TRACKING & MEASUREMENT PERFORMANCE

The Sentinel-3 POD receiver employs a fixed 10° elevation mask for tracking which has been selected based on the tracking sensitivity and the available number of tracking channels. As shown in Fig. 4, the tracked satellites are homogenously distributed on the celestial sphere within this limit.

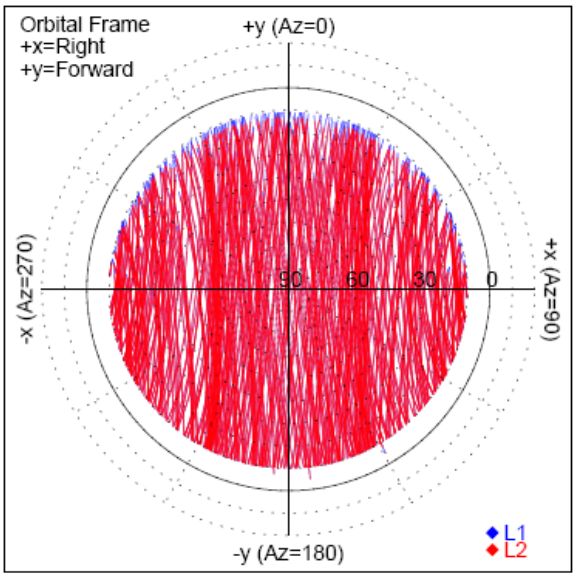

Fig. 4 Skyplot of tracked satellites

L1 C/A code tracking is generally acquired once a new satellite raises above the elevation threshold, whereas a small acquisition delay is obvious for the semi-codeless tracking on L2.

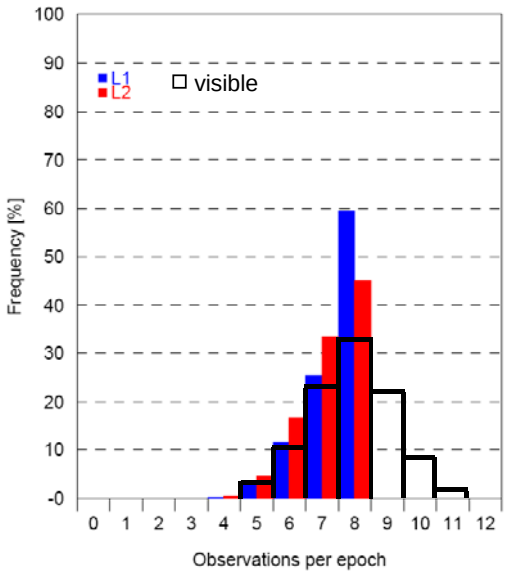

Fig. 5 Histogram of the number of tracked and visible satellites

Taking into account the limited number of channels, the number of tracked satellites is in good accord with the overall distribution of visible satellites above the elevation mask (Fig. 5). A total of 7-8 satellites is tracked on both L1 & L2 in about 78% of all epochs and only in very rare cases the number of tracked satellites sinks to the minimum of 4 required for a kinematic navigation fix.

At the simulated power levels, the carrier-to-noise-density varies between 37 dB-Hz and 51 dB-Hz for L1 C/A code tracking of Block-IIF satellites, while the semi-codeless P(Y) tracking achieves a C/N_0 between 11 and 39 dB-Hz.

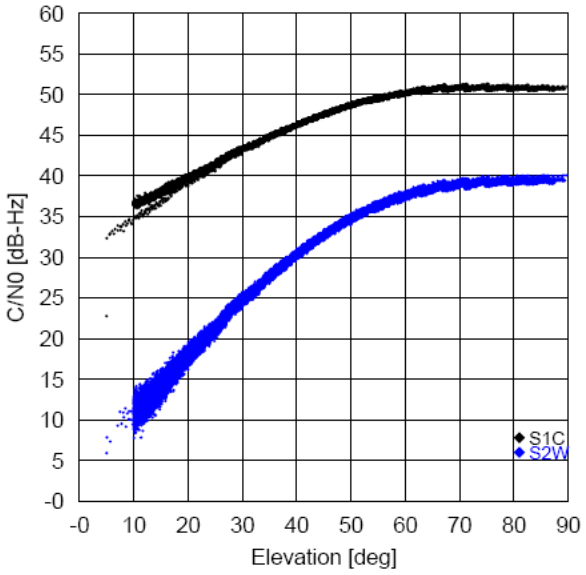

Fig. 6 Carrier-to-noise-density for L1 C/A and L1/L2 P(Y) tracking of simulated Block-IIF satellites

These values are in good accord with terrestrial measurements using a roof-top antenna (Fig. 7) but are most likely conservative for the space environment which yields higher C/N_0 values due to a much lower antenna noise temperature.

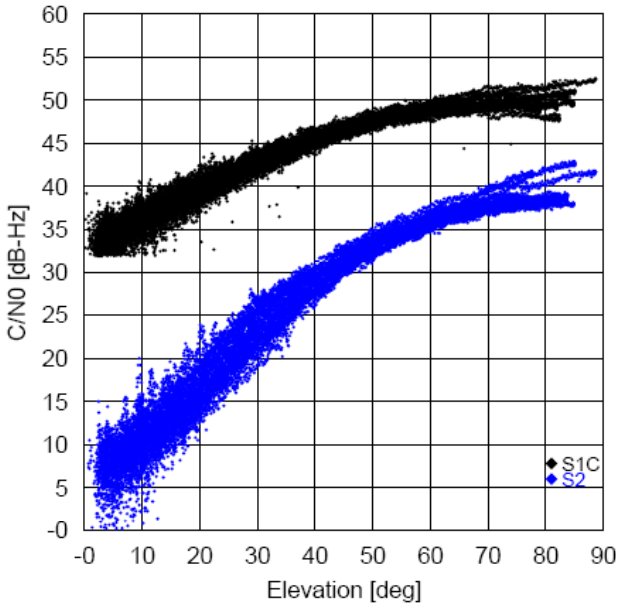

Fig. 7 Carrier-to-noise-density for L1 C/A and L1/L2 P(Y) tracking of GPS POD receiver measurements obtained in a ground test with a Sensor Systems S67-1575-14 antenna and chokering.

The semi-codeless tracking losses of the GPS POD receiver observed in the signal simulator test match the theoretical values for Z-tracking (see [15]) within about 0.5 dB, which confirms the validity of the C/N_0 values reported by the receiver.

For an analysis of the receiver noise, a virtual zero baseline test (cf. [9]) has been used. It resembles a traditional zero-baseline test but uses measurements collected with a single receiver unit in two independent runs of the same signal simulator scenario. The noise is then determined from measurement double differences formed for pairs of satellites with nearly equal C/N_0. For C/A and P(Y) pseudorange measurements the noise was, furthermore, derived from the multipath combination (i.e. a ionosphere-corrected code-carrier difference).

Results of the receiver noise analysis are summarized in Figs. 8. and 9 for code and carrier phase measurements, respectively. Compared to its predecessor, the GRAS instrument on MetOp (see [16]) the Sentinel-3 GPS POD receiver exhibits a notably smaller P(Y) code noise due to the use of a smaller tracking loop bandwidth and larger pre-correlation interval. At high elevations, a code noise of 10 cm (P(Y)) to 20 cm (C/A) is achieved, while the corresponding carrier phase noise amounts the 0.5 mm and 0.2 mm, respectively.

The observed variation of the tracking noise with C/N_0 was found to be in good accord with theoretical predictions ([17], [15]) for the design bandwidth of the respective tracking loops (0.5 Hz for L1 C/A DLL, 10 Hz and 0.25 Hz for L1 C/A and L2 P(Y) PLL).

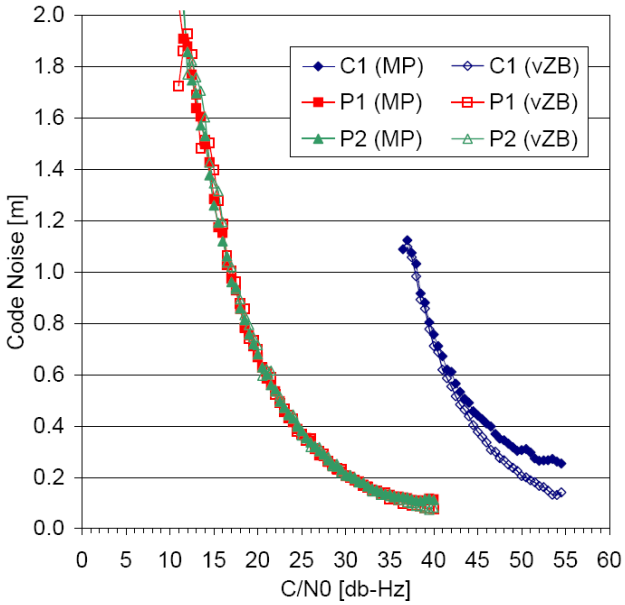

Fig. 8 Pseudorange noise versus carrier-to-noise-density for L1 C/A and L1/L2 P(Y) tracking. For C/A code, slightly different results were obtained using the multipath combination (MP) and the virtual zero baseline test (vZB).

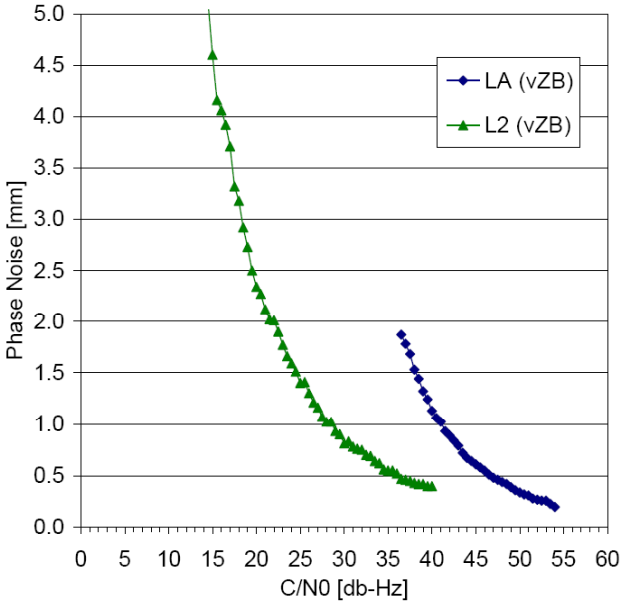

Fig. 9 Carrier phase noise versus carrier-to-noise-density for L1 C/A and L2 P(Y) tracking.

On average over the entire 24 h arc, a P(Y) pseudorange noise of about 0.55 m was obtained in the simulation, which results in a 1.6 m noise for the ionosphere-free pseudorange combination. The average C/A code noise amounts to 0.45 m. For carrier phase measurements the noise level of the ionosphere-free L1/L2 combination amounts to roughly 3 mm, which corresponds to a 1 mm noise on average for each individual frequency.

The absence of systematic errors in the raw measurements was further validated through a comparison of the code and carrier phase observations with the simulator truth values after differencing between channels to eliminate the receiver clock error (cf. [8], [9]). A sample result is given in Fig. 10 for L1 C/A code and phase measurements, which illustrates that potential systematic errors in the measurements are well below the noise level. In particular, no dependence on the line-of-sight velocity or acceleration can be observed.

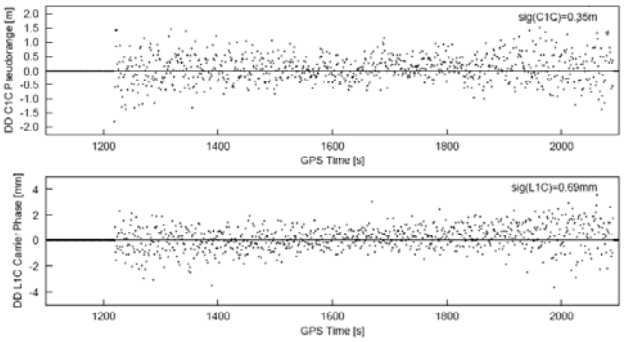

Fig. 10 Difference of measured and simulated L1 C/A code and phase observations for a pair of satellites with high relative line-of-sight dynamics.

Finally, the raw measurements collected in the simulation was processed in a reduced dynamics orbit determination software to assess the orbit reconstruction accuracy and the receiver contribution to the overall error budget. Assuming a perfect knowledge of the simulated GPS orbit and clock data, a 1.3 cm 3D rms position error (including 0.8 cm radial rms error) was achieved in this end-to-end test. The quoted values neglect other error sources such as ephemeris errors, attitude errors, or phase center uncertainties and are therefore not representative of the accuracy that can be achieved in the actual Sentinel-3 mission. However, they clearly indicate that the receiver performance is fully adequate to achieve the mission requirements for precision orbit reconstruction.

REAL-TIME NAVIGATION

While the real-time navigation system will ultimately be an integral part of the Sentinel-3 GPS receiver, the coding of the flight software has not yet been completed at this stage. The filter performance was therefore analyzed in post-processing with a stand-alone implementation of the same algorithms and making use of the raw GPS measurements recorded in the signal simulator test. Besides enabling a rapid and efficient tuning of the filter parameters, the RTNav software used for this purpose can also be used to process real flight data.

Maneuver-Free Case

To begin with the performance of the pseudorange-only filter is illustrated in Figs. 11-12. Both figures cover a period of roughly 24 h but ignore a 30 min arc after the filter initialization to illustrate the steady state performance of the filter. A 1.1 m 3D rms position error is achieved in this case, while the velocity solution is accurate to 1.1 mm/s. The radial component of the position solution, which is of primary relevance for the open loop altimeter operation is determined to better than 0.6 m and thus well within the mission requirement.

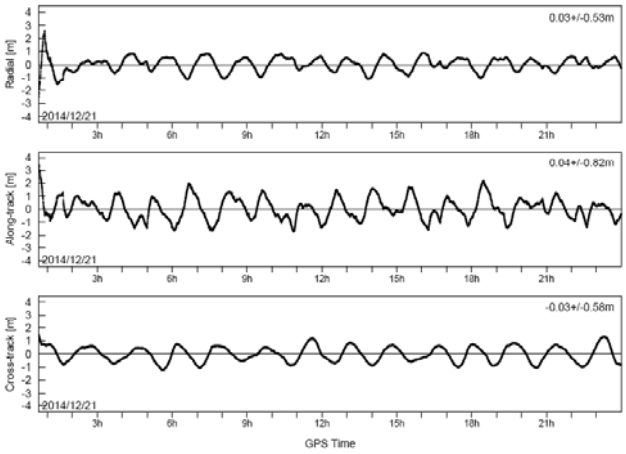

Fig. 11 Position error of the Sentinel-3 real-time navigation solution using a pseudorange-only filter.

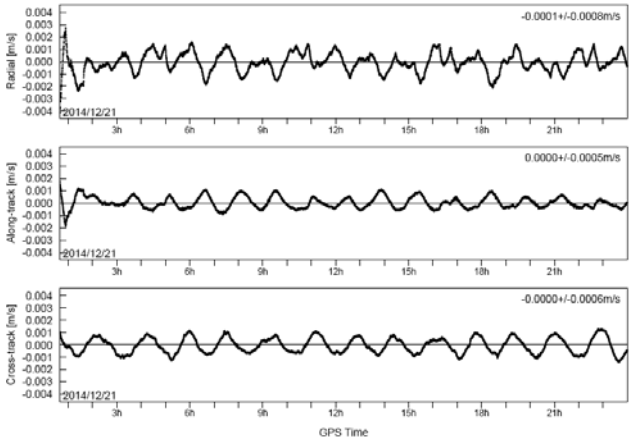

Fig. 12 Velocity error of the Sentinel-3 real-time navigation solution using a pseudorange-only filter.

Both the position and velocity solution exhibit a high level of smoothness over time scales of several minutes as a result of the dynamical filtering. Errors with a once-per-rev signature reflect the impact of uncompensated broadcast ephemeris errors that vary across the orbit as the set of tracked satellites changes.

Table 2 Sentinel-3 real-time navigation performance for pseudorange-only (PR) and pseudorange plus carrier phase (PR+CP) filter.

Type	R [m]	T [m]	N [m]	Pos [m]
PR	+0.03±0.53	+0.04±0.82	-0.03±0.58	1.13
PR+CP	+0.02±0.29	-0.07±0.40	-0.00±0.23	0.55

Compared to the pseudorange-only filter, which constitutes the baseline design for the Sentinel-3 navigation system, a factor of two performance

improvement can be achieved with a code+carrier filter (cf. Table 2). In both cases, the quality of the solution is dominated by the amplitude of the simulated broadcast ephemeris errors rather than the noise level of the employed measurements. However, the additional bias states considered in the code-carrier filter can partly absorb such errors and therefore enable a better overall navigation accuracy. The detrimental impact of broadcast ephemeris is further highlighted by the observation that a position error down to 3 cm 3D rms can be achieved with the same measurements and real-time navigation filter, if a perfect knowledge of the GPS orbit and clock data is assumed.

GRAS Flight Data Analysis

To confirm the suitability and validity of the employed broadcast ephemeris error model in the simulation, we have therefore independently processed GPS measurements from the GRAS instrument on MetOp-A using the true broadcast ephemerides available at the time of the measurements. The GRAS instrument shares various design elements with the GPS POD receiver for Sentinel-3 and exhibits a similar tracking performance. Furthermore, MetOp-A orbits the Earth at the same altitude as Sentinel-3. It is therefore well suited to assess the expected inflight-performance of the real-time navigation system.

Table 3 GRAS/MetOp real-time navigation performance for pseudorange-only (PR) and pseudorange plus carrier phase (PR+CP) filter using actual flight data for DOY 360 of 2006.

Type	R [m]	T [m]	N [m]	Pos[m]
PR	-0.04±0.53	+0.24±0.80	+0.00±0.37	1.06
PR+CP	-0.01±0.28	-0.03±0.46	-0.00±0.23	0.59

Results for a 24 h data arc in Dec. 2006 are shown in Table 3 and Fig. 13. As in the signal simulator test, a 30 x 30 gravity field model has been employed in the data analysis.

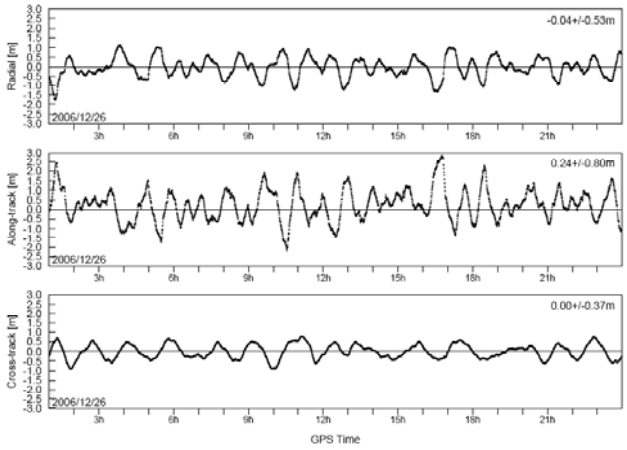

Fig. 13 Position error of the GRAS real-time navigation solution using a pseudorange-only filter.

The overall navigation performance is remarkably close to that obtained in the Sentinel-3 tests for both the pseudorange-only and the pseudorange plus carrier phase filter. This provides a further evidence for the proper performance of the filter and a supplementary justification for the employed model assumptions. A slightly different spectral characteristics of the position error may however, be noted as a result of slightly different filter settings employed for the GRAS data and the variation of the real broadcast ephemeris errors. For Sentinel-3, a final filter tuning is foreseen after launch to properly account for the inflight receiver performance and the broadcast ephemeris quality achieved with the latest enhancements of the GPS space and ground segment.

Start-Up Phase

The presentation of the real time navigation system has so far been focussed on the steady state performance of the filter. To complement this analysis, the filter behaviour during the start-up phase is now addressed in more detail.

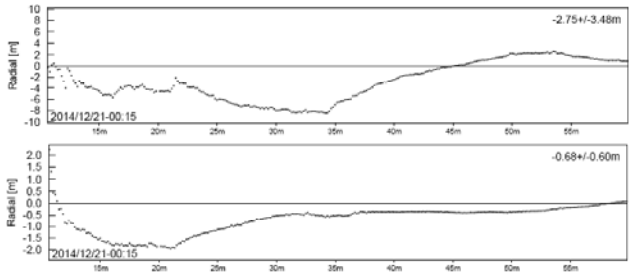

Fig. 14 Radial position error of the Sentinel-3 navigation filter during the initial 50 mins after initialization. *Top*: pseudorange-only filter. *Bottom*: code+carrier filter. Note the different scales of both graphs.

For illustration, the variation of the radial position error over half an orbital revolution after the initialisation is shown in Fig. 14 for both the filter with and without carrier phase measurements. Whereas the steady state performance of both filter concepts differs by a factor of two, a more pronounced difference is obvious during the start-up phase. Likewise, errors exceeding the steady state amplitude are obvious in the pseudorange-only filter for a larger time span than in the code+carrier filter.

Even though no effort has been made to rigorously define and quantify the begin of a steady-state phase, it is apparent that the use of carrier phase data contributes to a more rapid convergence of the filter after its initialisation. In the given example, radial errors of up to 2 m (i.e. more than 3 times the long-term rms error) occur for almost 45 min in case of the pseudorange-only filter, whereas the PR+CP filter achieves a radial error of less than 1 m within 15 min. Use of the advanced filter design is therefore beneficial for both the overall navigation accuracy and the rapid availability of high quality navigation data after the filter activation.

Maneuver-Inclusive Real-Time Navigation

We conclude the analysis with a discussion of the real-time navigation filter performance in the presence of orbital maneuvers. Even though such maneuvers occur only occasionally in a real mission, a 12h simulation has been conducted with a total of ten in-plane and out-of-plane corrections separated by one hour each. Details of the simulated maneuver parameters are given in Table 1.

When using both pseudorange and carrier phase measurements in the filter, only a small decrease of the positioning accuracy (0.7m 3D rms) compared to the maneuver-free case was obtained, despite the fact that no a priori information on the maneuver size was utilized (Fig. 15).

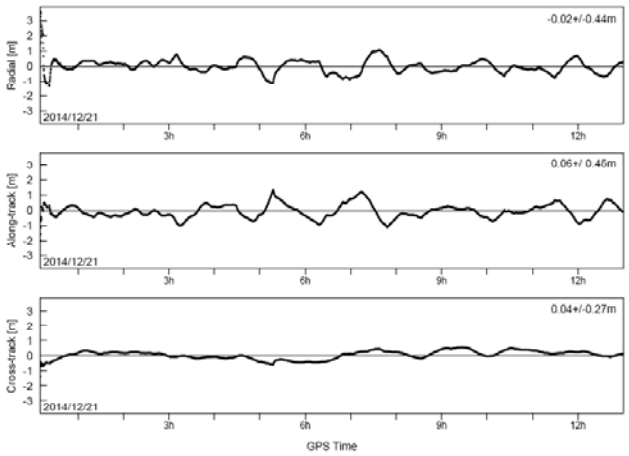

Fig. 15 Position error of the Sentinel-3 real-time navigation solution using code and carrier phase measurements in the presence of maneuvers.

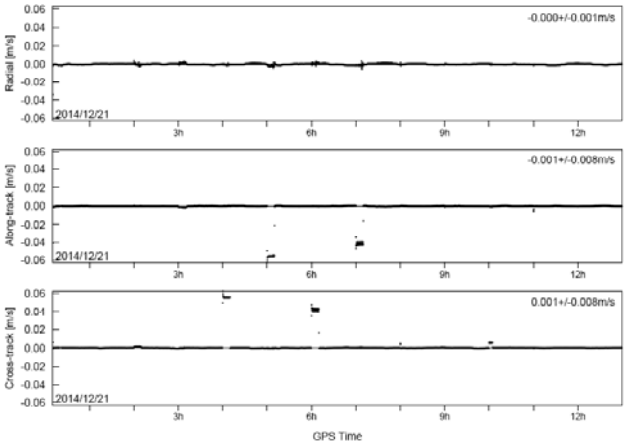

Fig. 16 Velocity error of the Sentinel-3 real-time navigation solution using code and carrier phase measurements in the presence of maneuvers.

The presence of maneuvers is obvious though, in the velocity solution, which is affected by systematic errors of up to 5 cm/s during the thrust arcs (Fig. 16). The occurrence of such velocity errors is a natural consequence of the fact that the filter acts as a first order filter during the maneuver period and responds with a steady state error proportional to the size of the unmodelled acceleration during this period. Outside the maneuvers, the velocity solution is again of similar quality as in the maneuver free case.

For the pseudorange-only filter, the presence of maneuvers affects the navigation accuracy in a more dramatic way than in the case discussed so far. Here an average position error of 3.8m 3D rms was obtained if no a priori information on the maneuver size was employed. Due to the highly kinematic behavior of the filter during the boost phase and the notable pseudorange noise, a notable scatter of the position solution is obvious during the maneuvers (Fig. 17). Likewise the slower convergence time of the filter results in a degraded performance in between the maneuvers.

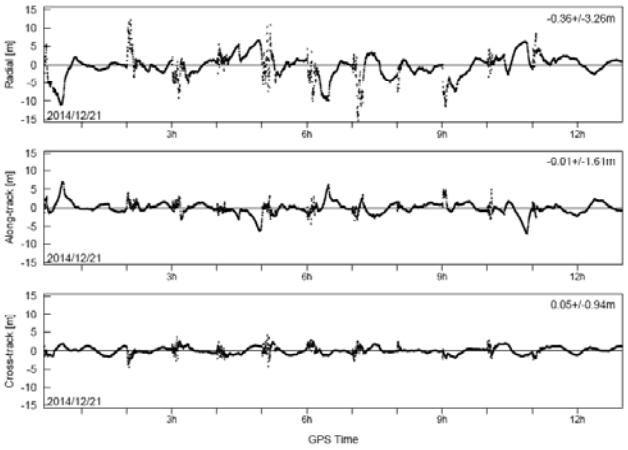

Fig. 17 Position error of the Sentinel-3 real-time navigation solution using only pseudorange measurements in the presence of maneuvers.

A performance improvement is obviously possible by making use of the a priori information on the thrust exerted during the maneuver. Assuming a maneuver execution error of up to 10%, the positioning accuracy can for example be improved to 3.3m in the given test case.

SUMMARY AND CONCLUSION

The Sentinel-3 GPS receiver and the design a real-time navigation filter design have been presented. Extensive signal simulator tests have been used to validate the tracking performance of the core receiver and the expected navigation accuracy of the real-time filter. It is demonstrated that a 1m 3D rms positioning accuracy and a better than 0.5 m radial accuracy can be achieved during routine operations even with a pseudorange-only filter. While this is well within the mission requirements, it has been shown that a factor of two performance improvement may be achieved with a filter employing both pseudorange and carrier phase measurements. Aside from an improved steady state accuracy, the advanced filter design benefits from a shorter start-up time and is more tolerant to maneuvers. Even though the maneuver

inclusive simulation represents an extreme and unrealistic case it helps to better understand the relative merits and weaknesses of the different filter concepts. For the actual Sentinel-3 mission, the pseudorange-only filter is currently considered as a baseline in view of its lean design and tight quality assurance requirements for the real-time flight software.

REFERENCES

[1] Aguirre M., Berruti B., Bezy J.-L., Drinkwater M., Heliere F, Klein U., Mavrocordatos C, Silvestrin P., Greco B., Benviste J; *Sentinel-3 – The Ocean and Medium-Resolution Land Mission for GMES Operational Services*; ESA Bulletin 131, Aug. 2007, pp. 25-30 (2007).

[2] Sust M., Carlström A., Garcia-Rodriguez A.; Spaceborne Dual Frequency GPS Receiving System for Science and Earth Observation; NAVITEC'2008, 10-12 Dec. 2008, Noordwijk (2008).

[3] Silvestrin P., Bagge R., Bonnedal M., Carlström A., Christensen J., Hägg M., Lindgren T., Zangerl F.; *Spaceborne GNSS Radio Occultation Instrumentation for Operational Applications*, ION-GPS-2000 Conference, Salt Lake City, 19-22 Sept. 2000, 872-880 (2000).

[4] Montenbruck O., Ramos-Bosch P.; *Precision Real-Time Navigation of LEO Satellites using Global Positioning System Measurements*; GPS Solutions **12/3**,187-198 (2008). DOI 10.1007/s10291-007-0080-x

[5] Montenbruck O., Markgraf M., Santandrea S., Naudet J., Gantois K., Vuilleumier P.; *Autonomous and Precise Navigation of the PROBA-2 Spacecraft*; AIAA 2008-7086; AIAA Astrodynamics Specialist Conference, 18-21 Aug. 2008, Honolulu, Hawaii (2008).

[6] Montenbruck O., Gill E.; *Satellite Orbits – Models, Methods and Applications*; Springer Verlag, Heidelberg; (2000).

[7] Montenbruck O., Gill E.; *State Interpolation for On-board Navigation Systems*; Aerospace Science and Technology **5**, 209-220 (2001). DOI 10.1016/S1270-9638(01)01096-3

[8] Montenbruck O., Holt G.; *Spaceborne GPS Receiver Performance Testing*; DLR-GSOC TN 02-04; Deutsches Zentrum für Luft- und Raumfahrt, Oberpfaffenhofen (2002).

[9] Montenbruck O., Garcia-Fernandez M., Williams J.; *Performance Comparison of Semi-Codeless GPS Receivers for LEO Satellites*; GPS Solutions **10**, 249-261 (2006). DOI 10.1007/s10291-006-0025-9

[10] Montenbruck O., van Helleputte T., Kroes R., Gill E.; *Reduced Dynamic Orbit Determination using GPS Code and Carrier Measurements*; Aerospace Science and Technology **9/3**, 261-271 (2005).

[11] Navstar GPS Space Segment/Navigation User Interfaces; NAVSTAR Global Positioning System Interface Specification IS-GPS-200 Rev. D, 7 Dec. 2004.

[12] Warren D. L. M., Raquet J. F.; *Broadcast vs precise GPS ephemerides: a historical perspective*, GPS Solutions **7**, 151–156 (2003).

[13] Creel T., Dorsey A. J., Mendicki P. J., Little J., Mach R.G., Renfro B. A.; *The Legacy Accuracy Improvement Initiative*, GPS World **17/3**,20 (2006).

[14] Van Dierendonck A. J.; GPS Receivers; chap. 8 in: Spilker J., Parkinson B., eds.; *Global Positioning System: Theory and Applications Vol. I*; American Institute of Aeronautics and Astronautics Inc., Washington (1995).

[15] Woo K.T.; *Optimum Semi-Codeless Carrier Phase Tracking of L2*; Navigation: Journal of the Institute of Navigation, **47(2),** pp. 82 (2000).

[16] Montenbruck O., Andres Y., Bock H., van Helleputte T., van den IJssel J., Loiselet M., Marquardt C., Silvestrin P., Visser P., Yoon Y.; *Tracking and Orbit Determination Performance of the GRAS Instrument on MetOp-A*; GPS Solutions **12/4**, 289-299 (2008). DOI 10.1007/s10291-008-0091-2

[17] Van Dierendonck A. J., Fenton P, Ford T; *Theory and Performance of Narrow Correlator Spacing in a GPS Receiver*; Proceedings of the ION NM-92, National Technical Meeting of The Institute of Navigation; San Diego, California, Jan. 27-29, 1992; pp. 115-124 (1992).